Title

TENSILE BEHAVIOR OF SUPERPIASTIC Al-Cu-Li-Zr ALLOY 2090 AT CRYOGENIC TEMPERATURES

Authors

Morris, J.W.
Nieh, T.G.

Publication Date

1987

Center for Advanced Materials

CAM REPORT

Presented at the International Cryogenic Materials Conference, St. Charles, IL, January 10–12, 1987

TENSILE BEHAVIOR OF SUPERPLASTIC Al-Cu-Li-Zr ALLOY 2090 AT CRYOGENIC TEMPERATURES

J. Glazer, J.W. Morris, Jr., and T.G. Nieh

January 1987

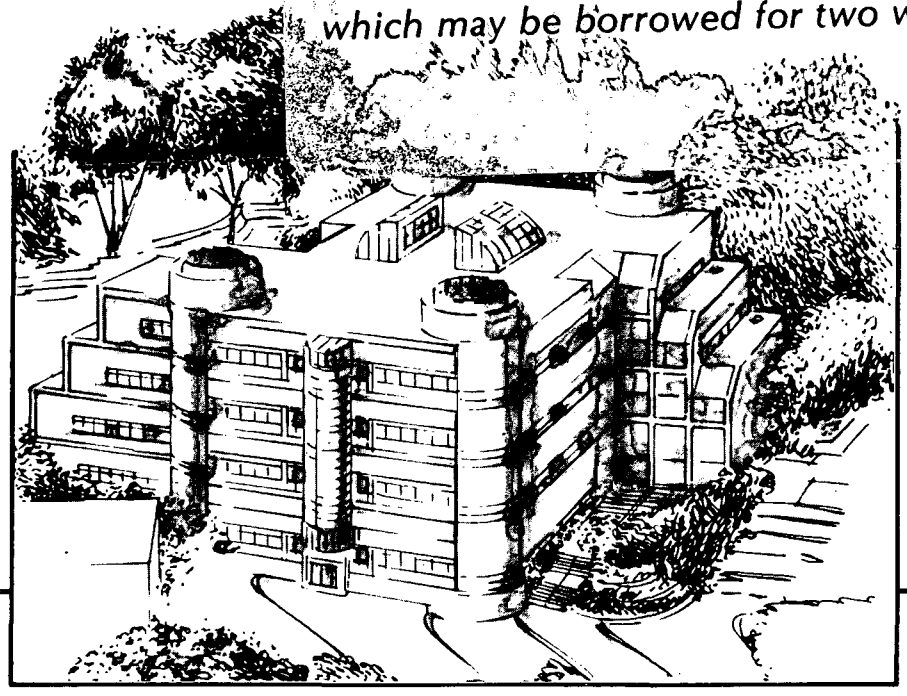

Materials and Chemical Sciences Division

Lawrence Berkeley Laboratory • University of California

ONE CYCLOTRON ROAD, BERKELEY, CA 94720 • (415) 486-4755

Prepared for the U.S. Department of Energy under Contract DE-AC03-76SF00098

DISCLAIMER

Tensile Behavior of Superplastic Al-Cu-Li-Zr Alloy 2090 at Cryogenic Temperatures

J. Glazer and J.W. Morris, Jr.

Center for Advanced Materials, Lawrence Berkeley Laboratory, and
Department of Materials Science and Mineral Engineering,
University of California, Berkeley, California

T.G. Nieh

Lockheed Palo Alto Research Laboratory
Palo Alto, California

ABSTRACT

The tensile behavior of superplastic Al-Cu-Li-Zr alloy 2090 sheet at cryogenic temperatures is investigated in both superplastically formed and unformed material. In both cases, the tensile properties improve significantly at low temperatures. The improvement in uniform elongation between room temperature and 4 K is especially large. As in other 2090 material with different microstructures, this improvement seems to be associated with increased strain hardening rates at low temperatures. A transition in tensile failure mode with decreasing temperature is also observed.

INTRODUCTION

Aluminum-lithium alloys have attracted a great deal of interest in the aircraft and aerospace industries because they have a lower density and higher elastic modulus than conventional aluminum alloys with similar combinations of mechanical properties.[1] The cryogenic properties of aluminum-lithium alloys are of interest primarily for fabrication of large liquid hydrogen (20 K), oxygen (90 K) or methane (110 K) fuel tanks used in modern space vehicles. In addition to the external tank of the space shuttle, which is constructed from an Al-Cu alloy, 2219-T87, large tanks are envisioned for the National Aero-Space Plane (NASP) and various heavy-launch vehicles.[2] Aluminum-lithium alloys are particularly appealing for these kinds of space applications because of the premium on reducing structural weight. Other potential applications at cryogenic temperatures include structural components of fusion or particle accelerator systems that employ 4 K superconductor magnet technology.

Previous work shows that both the strength-toughness relation and the tensile elongation of aluminum-lithium alloy 2090-T81 improve dramatically as temperature goes down.[3,4] Although a similar improvement in the mechanical properties of alloy 2219-T87 is observed at cryogenic temperatures, the improvement in 2090 properties is significantly

greater. Figure 1 compares the strength-toughness combinations of these alloys as a function of temperature. As shown in the figure, at 4 K, the mechanical properties of 2090-T81 are far superior to those of 2219.[3] A similar improvement in tensile properties is also observed for 2090 in the solution treated and quenched T4 temper.[5] The temperature variation of the elastic constants of 2090-T81 has also been studied; 2090-T81 maintains its stiffness advantage over conventional aluminum alloys over the range 298 K to 4 K.[6] On the basis of these data, various 2090 tempers are being considered for the applications described above. The cryogenic mechanical properties of other aluminum-lithium alloys are also being investigated.

Superplastic forming has also attracted considerable interest in the aerospace materials community because it allows efficient fabrication of complex parts and saves material. A number of aluminum-lithium alloys have been shown to behave superplastically after appropriate thermomechanical processing to achieve a fine recrystallized grain structure.[7] These materials generally have lower strengths than material in a largely unrecrystallized commercial temper such as alloy 2090-T81, even after solution treatment and aging to peak strength. This difference is attributed in part to the loss of textural and substructural strengthening and in part to the impossibility of performing a stretch to facilitate precipitation prior to aging of a formed part.

This paper investigates the tensile properties at cryogenic temperatures of sheet of 2090 composition after processing to create a superplastic microstructure and after superplastic forming.

EXPERIMENTAL PROCEDURE

Superplastic 2090 sheet of nominal composition Al-2.7Cu-2.2Li-0.1Zr (by weight percent) was produced as follows.[8] The starting material was cast by Reynolds Metals Company as 10 cm x 20 cm x 25 cm (4" x 8" x 10") ingot, homogenized for 24 hours at 537°C (1000°F) and rolled to 2 cm (0.8") thick plate. The actual composition of the material is Al-2.5Cu-2.3Li-0.2Zr. Additional processing was performed by the Lockheed Missiles and Space Company to produce superplastic material. The material was solution treated at 537°C (1000°F) for 1 hour, overaged at 396°C (745°F) for 16 hours, air-cooled to 287°C (550°F) and isothermally rolled at 287°C (550°F) to 2 mm (0.08") for a total true strain of -2.3. This processing sequence is typical of those used to provide the fine stable grain size required for superplasticity in aluminum alloys. The overaging step facilitates the introduction of a high dislocation density during the rolling step which, in turn, provides the numerous nucleation sites required to get a fine recrystallized structure when the temperature is raised (e.g. at the beginning of the forming process).

After thermomechanical processing, the 2090 sheet was superplastically formed at 485°C (905°F) into a headbox, a hat-shaped piece with a rectangular cross section. The headbox, the forming process and the superplastic behavior of the alloy are described in greater detail by Henshall, et al.[8] Tensile specimens were cut from the flange of the hat (ε = 0), and from the sides and top of the hat which were 0.5 mm (0.020 in) and 0.075 mm

(0.030 in) thick (ε = -3.68 and -3.28, respectively). Specimens were also cut from the unformed sheet. The sheet and flange specimens were approximately 2 mm (0.08") thick. The specimens were cut parallel to the original rolling direction. All specimens were solution treated 0.5 hours, quenched in 5% glycol in cold water, aged to approximately peak strength at 375°F (190°C) for 8 hours and air cooled before mechanical testing. The aging behavior is discussed further by Henshall, et al.

Tensile tests were performed using a subsize flat tensile specimen with a 2.54 cm (1.0 inch) gauge length. Elongations less than 20% were measured using an extensometer. Tests were performed on a servo-hydraulic testing machine equipped for cryogenic testing. Duplicate specimens were tested except at 4 K where all data points represent single specimens. All tests were conducted using a crosshead displacement rate of 2.1×10^{-3} cm/sec (0.05 in/min). Calculations of the strain hardening rate $d\sigma/d\varepsilon$ (where σ and ε are the true stress and strain, respectively) were made using the technique described in ref 5.

Optical microscopy was performed on specimens polished to 0.05 μm and etched using Keller's reagent.

RESULTS

The tensile properties of the material before and after superplastic forming to various strains are given in Table 1. The yield strength and ultimate tensile strengths at room temperature are in good agreement with those given by Henshall, et al. The room temperature elongations reported here are lower than those measured by Henshall, et al. on short gauge tensile specimens. Summary properties for 2090-T81 and 2090-T4 from ref. 5 are given for comparison. In general, these data show an improvement in properties at low temperature consistent with other results for 2090 in different microstructural conditions. Perhaps the most striking result is that although the room temperature elongation of all samples was small, the elongations and ultimate tensile strengths at low temperatures approach those of unrecrystallized 2090-T81 plate, albeit at lower strength levels.

Comparison of the properties of the base superplastic sheet material with formed material provides information on the effect of the superplastic forming step on final properties. At room temperature and 77 K, the plate material and the flange material have essentially identical properties, an expected result since in the absence of strain the superplastic forming step (485°C) has little influence on the mechanical properties of the sheet which is later solution treated at 537°C. The same reasoning suggests that the difference between them in 4 K strength and elongation is probably a result of specimen-to-specimen variation. The tensile properties of the 0.50 mm and 0.75 mm specimens provide insight into the effect of superplastic forming when the strain is significant. There appears to be a degradation of strength (~ 10%) associated with the forming process, but little effect on the tensile elongation. The behavior of formed material at 4 K deserves special mention. The low elongation recorded for 0.75 mm thick material represents a single specimen. It is not clear at this time whether the result of this test is spurious, and further study is in order.

Comparison of the strain hardening rate to the true stress as a function of true strain provides insight into tensile behavior in two ways: in ductile specimens that fail at the geometric instability point when the Considere criterion $d\sigma/d\varepsilon = \sigma$ is satisfied, differences in the strain hardening rate as a function of temperature or microstructure provide insight into the origins of elongation and ultimate tensile properties, and in specimens that fail early due to internal flaws the strain hardening rate - strain plot makes it possible to compare the early behavior of these specimens with those that failed at instability. All specimens tested at 4 K displayed serrated yielding. Strain hardening rates for these specimens were calculated using the outer envelope of the stress-strain curve. The elongation and tensile strength values presented in Table 1 are conservative estimates of the actual properties since the majority of the specimens failed near the extensometer pins before a peak load was achieved. However, comparison of the strain hardening rate to the true stress indicates that the only specimen that failed well before geometric instability was the 0.75 mm specimen tested at 4 K. Figure 2 shows the effect of temperature on the strain hardening rate of unformed superplastic sheet. Similar data were generated for sheet formed to 0.75 mm (0.030 in). In both cases, the strain hardening rate increases with decreasing temperature. This increase is associated with an increase on tensile elongation since the geometric instability that leads to necking is deferred. In addition, the strain hardening rates essentially superimpose at all three temperatures. The specimen tested at 4 K that failed after 2% strain has an initial strain hardening rate equivalent to that of the sheet specimen that elongated 25%. This suggests that this specimen failed due to an internal flaw rather than due to a catastrophic increase in brittleness between 77 K and 4 K.

The grain structure of the superplastic sheet after solution treatment is illustrated in Figure 3. The grains are approximately equiaxed in the LT plane and approximately 5 μm in size following recrystallization that would normally occur during the superplastic forming step (here during solution treatment). However, there is some retention of the prior hot worked grain structure of long flat "pancake" grains. Examination of the macrostructure also reveals the presence of hard second phase particles several microns in size that were not dissolved during the solution treatment. The distribution of these intermetallic particles in formed and unformed material has been studied in more detail by Henshall, et al. These particles probably provide fracture initiation points.

Any variation in the tensile failure mode should also provide some insight into the variation of mechanical properties with temperature. The most obvious difference is that all specimens tested at room temperature failed in shear at 45° to the tensile axis, whereas specimens tested at low temperatures exhibited flat fracture surfaces. The overall appearance of the fracture surfaces is illustrated in Figure 4. The transition in failure mode from the shear fracture at room temperature to a flat intergranular fracture at 4 K is illustrated by the scanning electron micrographs in Figure 5. The failure at liquid nitrogen appears to be a mixture of the two failure modes.

DISCUSSION

The data presented here may be usefully compared with results for other material of 2090 composition in different microstructural conditions. Most previous work on cryogenic properties of this alloy describes the behavior of 2090-T81, an unrecrystallized grain structure made up of large elongated flat grains that contain a fine subgrain structure. To achieve the T81 temper, the material is stretched 6-8% before aging to peak strength. The 2090-T4 material described in reference 5 was prepared by solution heat treating and quenching 2090-T81. Although the trends in tensile behavior as a function of temperature for superplastic 2090 reported here are similar to those observed in unrecrystallized 2090, the improvements in behavior are much more dramatic. While the size of the improvement is at least in part due the relatively poor room temperature properties (especially elongation), the magnitude of the improvement is nonetheless striking.

The strain hardening rate behavior of superplastic 2090 is also similar to unrecrystallized 2090 at least insofar as it reproduces the association between increased strain hardening rates and increased elongation at low temperatures. Both materials show a distinct tendency to fail at the tensile instability point with little or no necking. Ongoing research at our laboratory is focussed on understanding the metallurgical sources of the increased strain hardening rates at low temperature. The qualitative similarity of the effect of temperature on tensile properties in the three microstructural conditions of 2090 examined to date suggests that the effect is relatively insensitive to microstructure.

The fracture mode transition observed in this material is not observed in unrecrystallized 2090. Presumably this change in fracture behavior has implications for the effect of temperature on the toughness of superplastic material, but this point has not been investigated.

CONCLUSIONS

The tensile behavior at cryogenic temperatures of alloy 2090 sheet thermomechanically processed to produce superplastic behavior was investigated before and after superplastic forming. Both formed and unformed material displayed large improvements in tensile behavior at cryogenic temperatures, especially in ultimate tensile strength and uniform elongation. The properties of 2090 superplastic sheet at 4 K approach those of 2090-T81, the best cryogenic aluminum alloy currently commercially available. The correlation between increased strain hardening rates at low temperatures and improved tensile elongation observed for unrecrystallized 2090 is also observed in superplastic sheet.

ACKNOWLEDGEMENTS

The authors would like to thank Ms. C. Henshall, Ms. C. McNally, and Dr. J. Wadsworth, Lockheed Missiles and Space Corporation, Lockheed Palo Alto Research

Laboratory for supplying materials and assistance during the course of this study. This study was jointly funded by the Lockheed Independent Research Program and the Director, Office of Energy Research, Office of Basic Energy Science, Material Sciences Division of the U.S. Department of Energy under Contract No. DE-AC03-76SF00098. J. Glazer is supported by an AT&T Bell Laboratories Fellowship.

REFERENCES

1. "Aluminium-Lithium Alloys III," C. Baker, P.J. Gregson, S.J. Harris and C.J. Peel, eds., The Institute of Metals, London (1986).
2. See for example, C. Covault, X-30 Research Narrowing Down Hypersonic Design Options, Aviation Week and Space Tech., April 27, 1987, p. 32.
3. J. Glazer, S.L. Verzasconi, E.N.C. Dalder, W. Yu, R.A. Emigh, R.O. Ritchie and J.W. Morris, Jr., Cryogenic Mechanical Properties of Al-Cu-Li-Zr Alloy 2090, Adv. Cryo. Eng., 32:397 (1986).
4. R.C. Dorward, Scripta Met. 20:1397 (1986).
5. J. Glazer, S.L. Verzasconi, R.R. Sawtell, and J.W. Morris, Jr., Mechanical Behavior of Aluminum-Lithium Alloys at Cryogenic Temperatures, Metall. Trans., in press (1987).
6. J. Glazer, J.W. Morris, Jr., S.A. Kim, M.W. Austin and H.M. Ledbetter, Temperature Variation of the Elastic Constants of Aluminum Alloy 2090-T81, AIAA J., in press (1987).
7. J. Wadsworth, C.A. Henshall and T.G. Nieh, Superplastic Al-Li Alloys, in: "Aluminium-Lithium Alloys III," C. Baker, P.J. Gregson, S.J. Harris and C.J. Peel, eds., p. 190, The Institute of Metals, London (1986).
8. C.A. Henshall, J. Wadsworth, M.J. Reynolds and A.J. Barnes, Design and Manufacture of a Superplastic-Formed Aluminum-Lithium Component, submitted to Materials and Design.

Table1. Tensile properties of 2090 sheet before and after superplastic forming to various strains. Data for 2090-T81 and 2090-T4 are taken from ref. 5.

Specimen	Test Temp. (K)	σ_y MPa (ksi)	σ_{uts}[¥] MPa (ksi)	uniform elong. %
Sheet	298	315 (46)	415 (60)	4.2
	77	350 (51)	510 (74)	11.3
	4	415 (60)	690 (100)	25
Flange	298	310 (45)	405 (58.5)	4.4
	77	345 (50)	510 (74)	13.4
	4	370 (54)	600 (87)	17
0.75 mm	298	285 (41)	380 (55)	5.1
	77	315 (46)	480 (70)	10.5
	4	370 (54)	450 (65)	2
0.50 mm	298	260 (38)	360 (52)	4.8
	77	275 (40)	>415 (60)†	>5.6†
2090-T81	298	455 (66)	490 (71)	6
	77	535 (78)	625 (91)	14
	4	535 (78)	650 (95)	20
2090-T4	298	120 (17)	270 (39)	19
	77	155 (23)	350 (51)	29
	4	190 (28)	435 (63)	25

¥ Engineering stress computed from highest measured load.
† Specimen thickness along gauge length was uneven. Elongation was non-uniform.

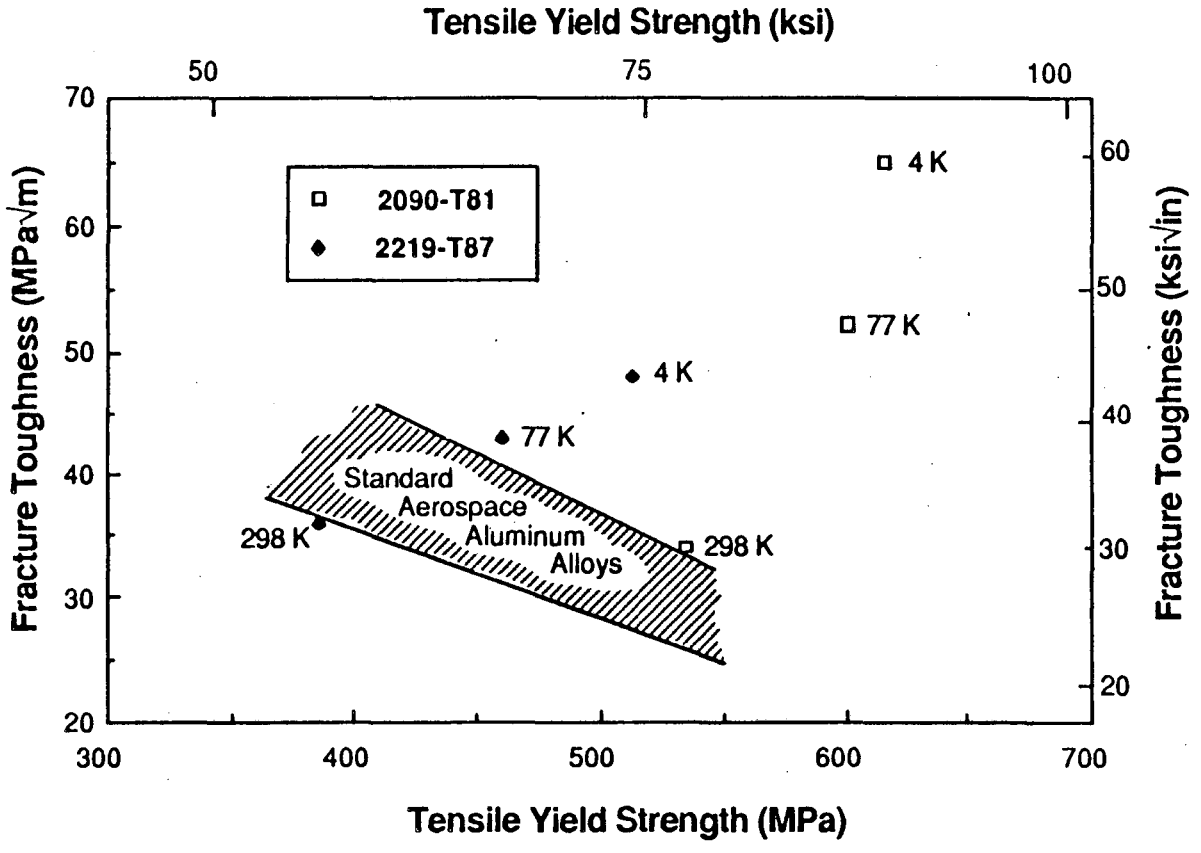

Figure 1. Comparison of the strength-toughness combinations for 2090-T81 and 2219-T87 plate as a function of temperature. Tensile data were determined from longitudinally oriented specimens; K_{Ic} values are calculated from J_{Ic} values for L-T compact tension specimens. Taken from ref. 3.

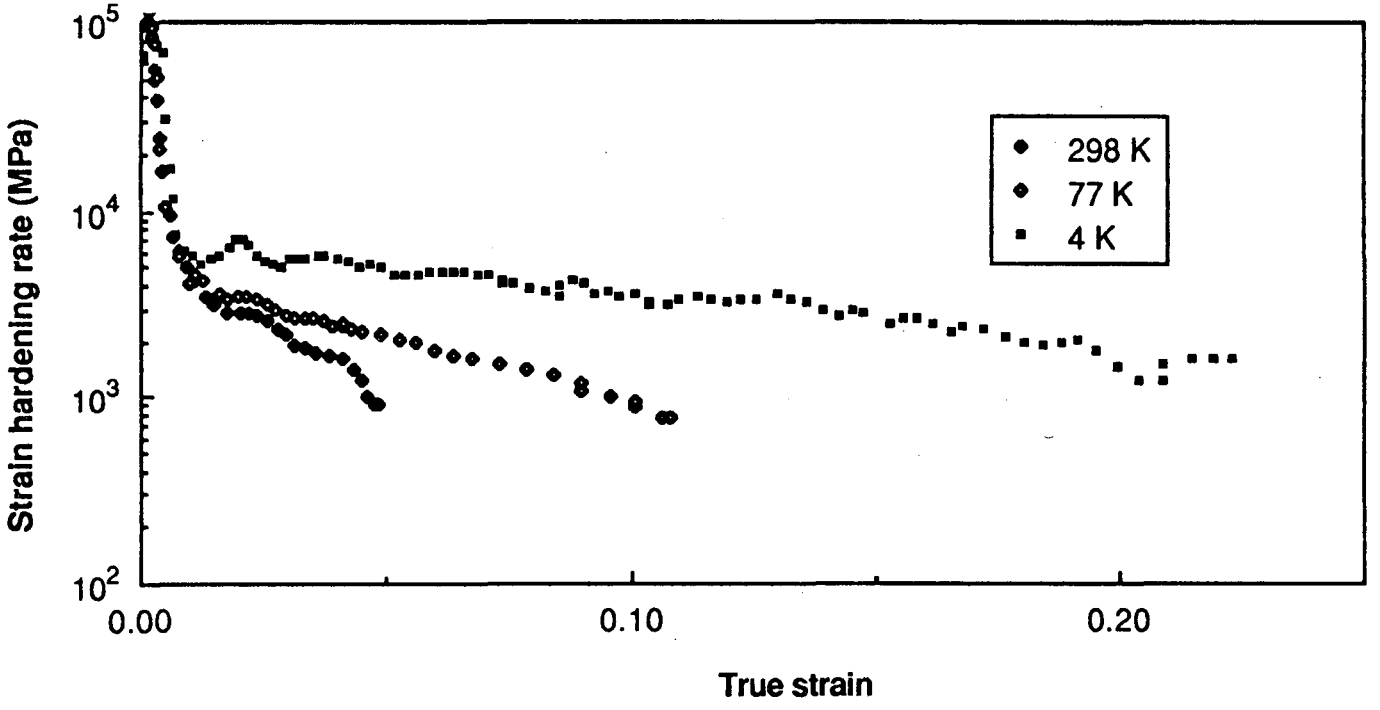

Figure 2. Strain hardening rate as a function of true strain at room temperature, 77 K and 4 K for unformed superplastic 2090 sheet.

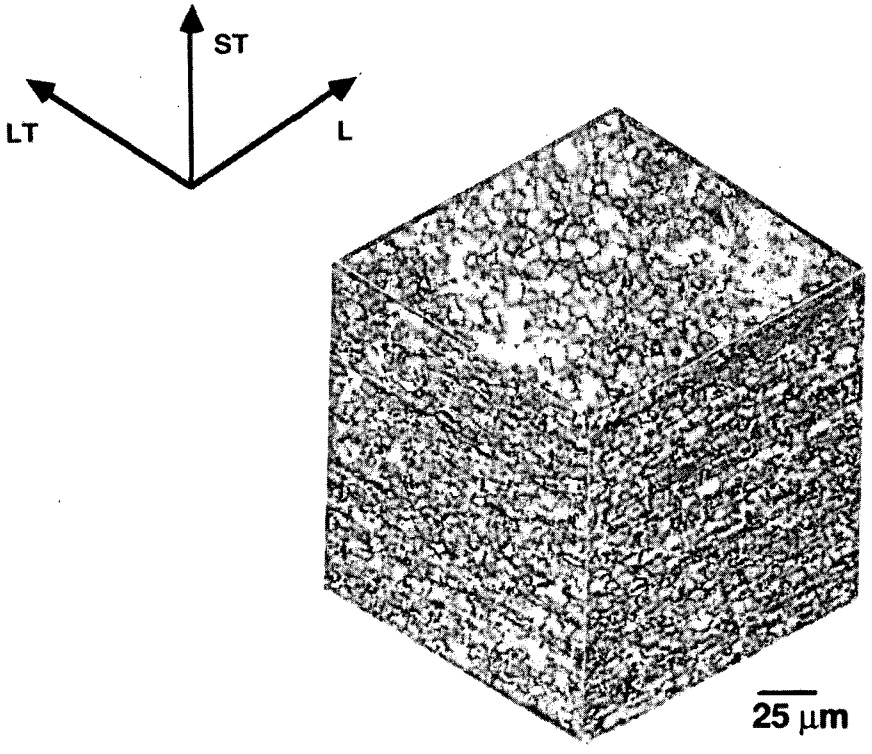

Figure 3. Optical micrograph illustrating the grain structure of superplastic 2090 after recrystallization.

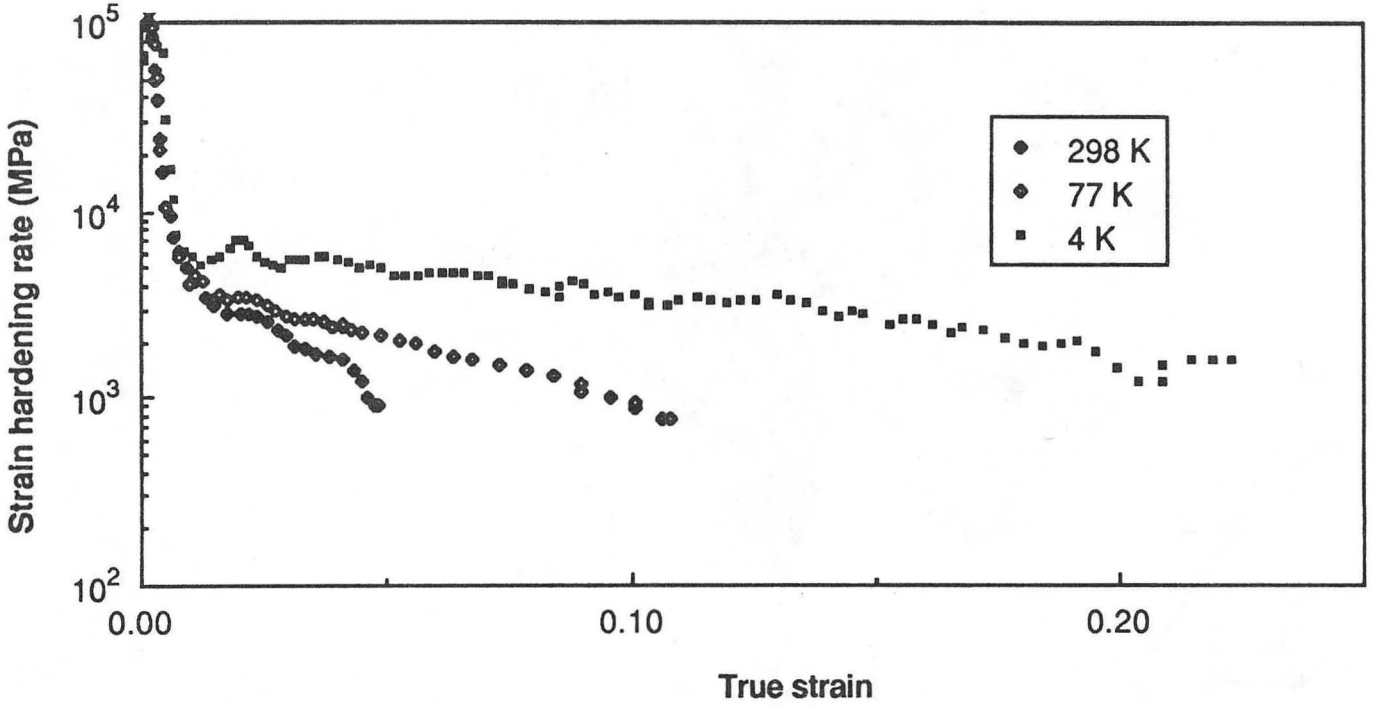

Figure 2. Strain hardening rate as a function of true strain at room temperature, 77 K and 4 K for unformed superplastic 2090 sheet.

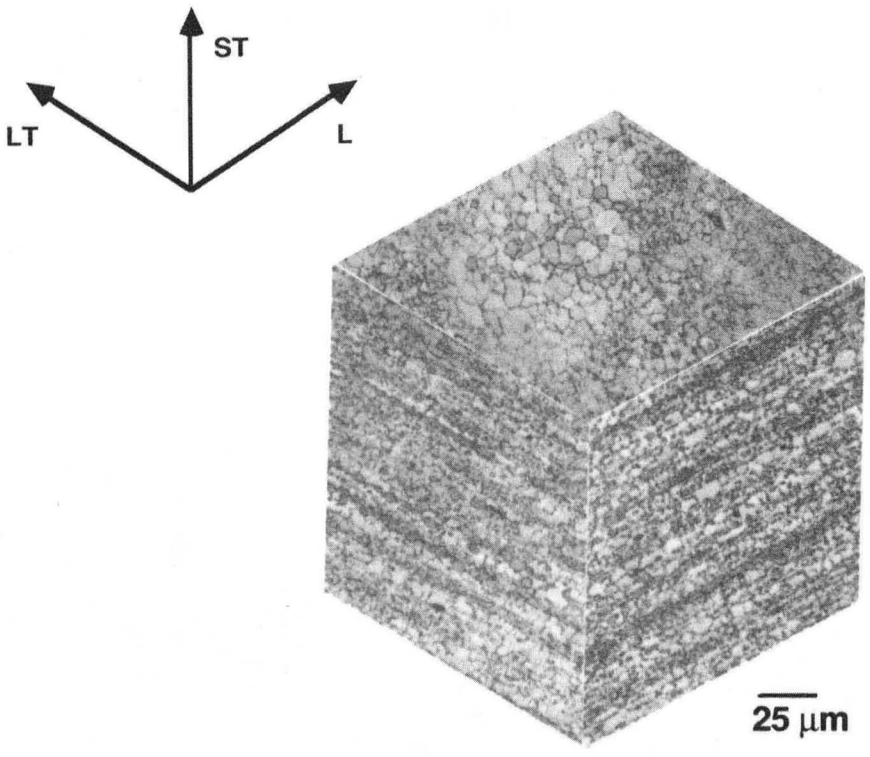

XBB875-3948

Figure 3. Optical micrograph illustrating the grain structure of superplastic 2090 after recrystallization.

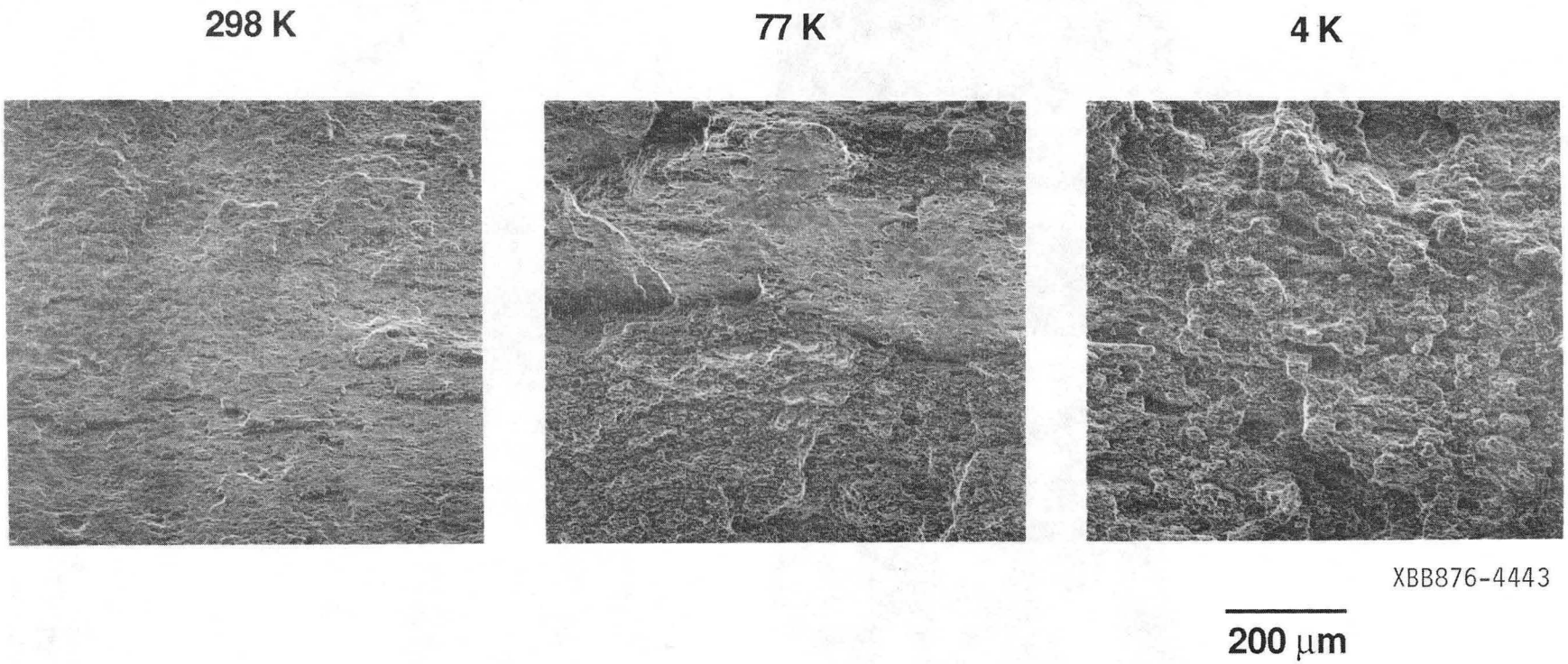

Figure 4. Overall tensile failure appearance of unformed superplastic 2090 sheet after testing at the indicated temperatures.

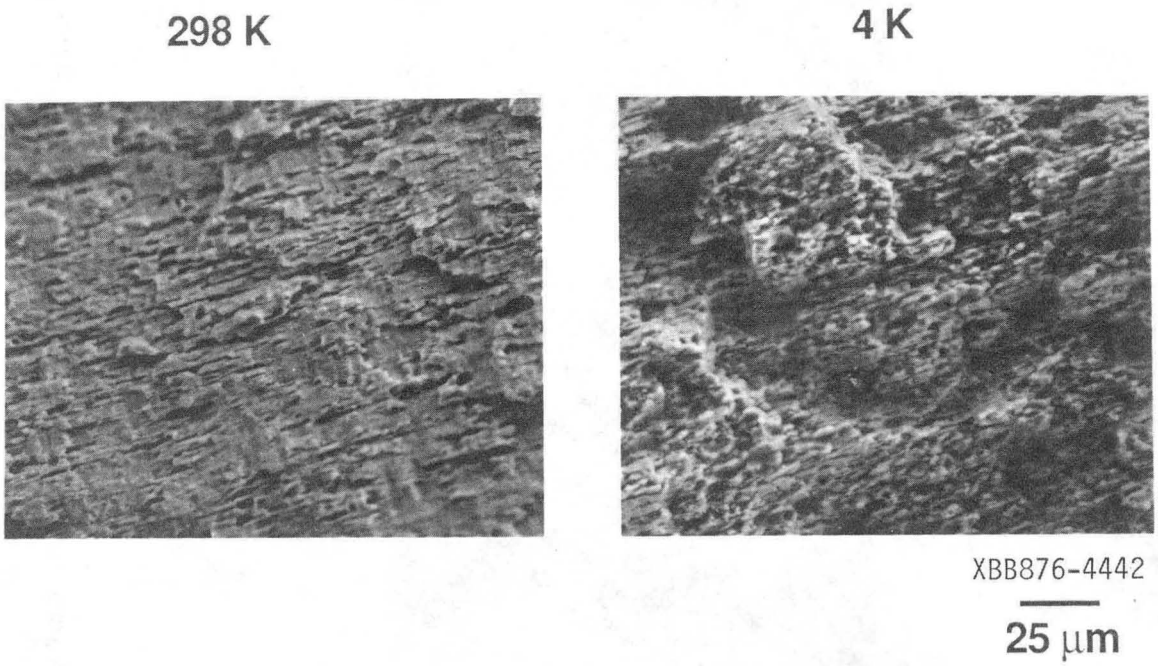

Figure 5. Comparison of the dominant tensile failure modes at room temperature and 4 K in unformed superplastic sheet.

LAWRENCE BERKELEY LABORATORY
TECHNICAL INFORMATION DEPARTMENT
UNIVERSITY OF CALIFORNIA
BERKELEY, CALIFORNIA 94720